Korean J. Chem. Eng., 36(6), 942-953 (2019)
DOI: 10.1007/s11814-019-0267-1

pISSN: 0256-1115
eISSN: 1975-7220

Adsorption of *p*-chlorophenol and *p*-nitrophenol in single and binary systems from solution using magnetic activated carbon

Yachan Rong and Runping Han†

College of Chemistry and Molecular Engineering, Zhengzhou University,
No 100 of Kexue Road, Zhengzhou, 450001 P. R. China
(*Received 19 November 2018 • accepted 8 April 2019*)

Abstract−Magnetic activated carbon (MAC) was prepared by co-precipitation. These particles had attractive adsorption capacity and could be easily separated from aqueous. MAC was used as adsorbent to remove *p*-chlorophenol (*p*-CP) and *p*-nitrophenol (*p*-NP) from solution in single and binary systems. In a single system, the equilibrium time was 60 min, the best initial pH was 3-8 and 3-6 for *p*-CP or *p*-NP adsorption, respectively. The existence of salt ions had little influence on the adsorption process, while surfactant had negative influence. The adsorption quantity from experiments was up to 97.3 $mg \cdot g^{-1}$ for *p*-CP and 116 $mg \cdot g^{-1}$ for *p*-NP at 293 K, respectively. Freundlich model and pseudo-second-order kinetic model fitted well the adsorption behavior. Thermodynamic parameters were calculated and the results showed that the process was spontaneous, exothermic and entropy production in nature. In addition, *p*-CP or *p*-NP-loaded MAC could be well reused by 0.01 $mol \cdot L^{-1}$ sodium hydroxide solution as regeneration agent. Kinetic process of desorption was fitted best by pseudo-second-order kinetic model. Results from the binary system showed that competitive adsorption existed during the process, and *p*-NP adsorption on MAC was easier than *p*-CP. Freundlich model well fitted the adsorption behavior in the binary system. Hydrogen-bonding, electron donor-acceptor and π-π interactions may be the main mechanisms of adsorption. MAC proved to be an excellent adsorbent for the removal of *p*-CP and *p*-NP from solution.

Keywords: Magnetic Activated Carbon, *p*-Chlorophenol, *p*-Nitrophenol, Competitive Adsorption, Desorption

INTRODUCTION

Phenolic hydrocarbons, including *p*-chlorophenol (*p*-CP) and *p*-nitrophenol (*p*-NP), are common pollutants found particularly in oil refineries, olive mills, plastics, pharmaceutical, steel industries [1-4]. Due to their harmful effect on humans and animals, many treatment technologies have been implemented to remove them from water, such as electrochemical oxidation [5], reverse osmosis [6], membrane separation [7], chemical coagulation [8], photodegradation [9] and adsorption [10,11]. Among these, adsorption is quite extensively used because of its simplicity, high efficiency, and without chemical addition [12,13]. Activated carbon is outstanding as adsorbent. Powdered activated carbon has large specific surface, but the properties of powder hinder its application in adsorption. In adsorption, powdered activated carbon easily leads to blockage of filter mesh and loss of adsorbent. How to quickly and effectively separate powdered activated carbon has become the key problem during the application of activated carbon in adsorption [14,15].

To solve these problems, magnetic technology was used in the adsorption while activated carbon served as the adsorbent. Yang et al. [16] synthesized magnetic Fe_3O_4-activated carbon nanocomposite by modified impregnation method to remove methylene blue. Singh et al. [17] prepared magnetic activated carbon using impregnation method to remove malachite green. Han et al. [18] produced magnetically modified activated carbon using co-precipitation technique and the carboxylic acid vapor treatment technique to remove *p*-NP. The magnetic activated carbon was also prepared using co-precipitation in our previous work to remove malachite green and the adsorption capacity at 303 K could reach up to 766 $mg \cdot g^{-1}$ [19].

Magnetic activated carbon (MAC) has the characterization of magnetic particles and activated carbon [20]. Moreover, MAC can be easily separated by commercial magnet [21,22]. Considering the complexity of actual wastewater, pollutants often coexist in sewage; competitive adsorption of phenolic compounds was performed on various adsorbents [23-25]. But the kinetic process of desorption was seldom studied. However, the methods of competitive adsorption can be improved.

In this work, MAC was used as adsorbent to remove *p*-CP and *p*-NP from solution, and adsorption property toward *p*-CP and *p*-NP was presented. The adsorption process of *p*-CP or *p*-NP on MAC in single system was performed, including dose of adsorbent, contact time, initial pH, coexisting ions, adsorption temperature and initial concentration. Kinetic models were used to fit the experimental data. Kinetic process of desorption and regeneration of spent MAC was also presented. In addition, competitive adsorption behavior between *p*-CP and *p*-NP in binary system was ex-

†To whom correspondence should be addressed.
E-mail: rphan67@zzu.edu.cn

plored to better study the adsorption capacity of MAC in mixtures.

MATERIAL AND METHODS

1. Materials

The chemicals used in testing were the following: ferric chloride ($FeCl_3$, Fengchuan Chemical Reagent, Tianjin, China), ferrous sulfate ($FeSO_4$, Sinopharm Chemical Reagent, Shanghai, China), ammonium hydroxide (25%-28%, w/w, Sinopharm Chemical Reagent, Shanghai, China), sodium chloride (NaCl, Kermel, Tianjin, China), sodium laurylsulfonate (SLS, Kermel, Tianjin, China), calcium chloride ($CaCl_2$, Kermel, Tianjin, China), cetyltrimethyl ammonium bromide (CTAB, Sinopharm Chemical Reagent, Shanghai, China), absolute ethanol (Fuchen Chemical Reagent, Tianjin, China), polyethylene glycol-6000 (Sinopharm Chemical Reagent, Shanghai, China), *p*-chlorophenol (*p*-CP, Aladdin, Tianjin, China) and *p*-nitrophenol (*p*-NP, Aladdin, Tianjin, China). All chemicals were of analytical grade and used without further purification. Distilled water was used. Activated charcoal was purchased from Macklin Company (Shanghai, China).

2. Preparation and Characterization of Magnetic Activated Carbon (MAC)

MAC was prepared by a simple co-precipitation method, and the process is described in our previous study [19]. Mixed iron salts were dissolved in distilled water under polyethylene glycol as dispersant, then activated carbon was added, followed by ammonia solution to precipitate, and the magnetic adsorbent was prepared.

Various methods were used to characterize MAC. The zero point of charge of MAC was nearly 7.1, and the results showed that the adsorbent surface was positively charged at pH<7.09 and negatively charged at pH>7.09. The results of XRD and TGA suggested that γ-Fe_2O_3 were the main magnetic phase and the content of activated carbon in MAC was about 50%. The results of Boehm titration showed that the surface of MAC contained abundant functional groups related to oxygen. The surface area of MAC was calculated by BET surface area and the surface area of MAC was 1.13×10^3 $m^2\cdot g^{-1}$ which indicated abundant pore structure. The morphology of MAC obtained by SEM and showed that MAC demonstrated a granular microstructure with irregular shaped grain, and the size of most particles was less than 1 μm. Magnetic hysteresis loops analysis of MAC showed that the saturation magnetization (Ms) was 5.20 emu·g^{-1} and could be separated from solution by external magnet [16,19].

3. Adsorption Experiments

Batch adsorption experiments with 10 ml *p*-CP or *p*-NP solution and 0.01 g MAC were carried out, including the adsorbent dose (1-20 mg, $C_{0,p\text{-CP or }p\text{-NP}}$=100 mg·$L^{-1}$), contact time (2-90 min, $C_{0,p\text{-CP or }p\text{-NP}}$=100 mg·$L^{-1}$), initial pH (3-12) of solution ($C_{0,p\text{-CP or }p\text{-NP}}$= 100 mg·$L^{-1}$), coexisting ions (NaCl, Na_2SO_4, CTAB and SLS, $C_{0,p\text{-CP or }p\text{-NP}}$ =100 mg·L^{-1}), adsorption temperature (293, 303, 313 K) and initial concentration ($C_{0,p\text{-CP or }p\text{-NP}}$=70-140 mg·$L^{-1}$). Adsorbent was separated by external magnet after adsorption. Concentrations of *p*-CP or *p*-NP in solution were measured on a UV/Vis-3000 spectrophotometer (Shimadzu Brand UV-3000 with a 1 cm path length) according to Lambert-Beer Law at a wavelength of maximum adsorbance of 225 nm for *p*-CP and 318 nm for *p*-NP, respectively.

The competitive adsorption of *p*-CP and *p*-NP involved two parts: 1) Fixing the concentration of *p*-CP (C_0=100 mg·L^{-1}) and changing the concentration of *p*-NP (C_0=70-140 mg·L^{-1}). The same method was also used to investigate the removal capacity of *p*-NP at the presence of *p*-CP; 2) Fixing the total concentration of *p*-CP and *p*-NP was 200 mg·L^{-1}. The concentration range of *p*-CP and *p*-NP changed from 0-200 mg·L^{-1} and 200-0 mg·L^{-1}, respectively. The adsorption isotherms of *p*-CP (*p*-NP) at the presence of different concentrations of *p*-NP (*p*-CP) were also studied.

For binary system, the concentrations of *p*-CP and *p*-NP were measured using the following formula:

$$A_{225}=k_{225}\,C_{p\text{-CP}}+k'_{225}\,C_{p\text{-NP}} \tag{1}$$

$$A_{318}=k_{318}\,C_{p\text{-NP}} \tag{2}$$

where A_{225} and A_{318} are adsorbance at 225 nm and 318 nm, respectively; k_{225} (L·mg^{-1}) and k'_{225} (L·mg^{-1}) are adsorption coefficients at 225 nm for *p*-CP and *p*-NP, respectively; k_{318} (L·mg^{-1}) is adsorption coefficient of *p*-NP at 318 nm. Then concentrations of *p*-CP and *p*-NP in mixed-solution can be calculated according to Eq. (1) and (2) if values of A_{225} and A_{318} are obtained.

The data obtained from adsorption test in batch mode were used to calculate the *p*-CP or *p*-NP uptake quantity. The quantity of *p*-CP or *p*-NP adsorbed onto unit weight of adsorbent (q, mg·g^{-1}) and the removal efficiency (*p*, %) were calculated using the following equations, respectively:

$$q=\frac{V(C_0-C)}{m} \tag{3}$$

$$p=\frac{(C_0-C_e)}{C_0}\times100\% \tag{4}$$

where C_0 is the initial concentration (mg·L^{-1}), C or C_e (mg·L^{-1}) is the concentration at any time or equilibrium, V is the reaction solution volume (L), and m is the mass of MAC (g).

4. Desorption and Regeneration Experiments

The regeneration capacity of spent or exhausted MAC was investigated in batch mode. Different desorbing solutions were chosen to desorb *p*-CP-loaded MAC (*p*-CP-MAC) or *p*-NP-loaded MAC (*p*-CP-MAC) (t=60 min, adsorbent dose=1 g·L^{-1}, C_0=100 mg·L^{-1}, T=303 K) and microwave method also used for regeneration. After desorption, the used MAC was reused to adsorb *p*-CP or *p*-NP and the adsorption condition was same with the first adsorption process. Then the best desorbing solution was chosen for the continuous desorption-adsorption studies to explore the reuse capacity of MAC. The desorption efficiency (D) and regeneration efficiency (η) were calculated in the following:

$$D=\frac{m}{m_c}\times100\% \tag{5}$$

$$\eta=\frac{q_n}{q_e}\times100\% \tag{6}$$

where D is the desorption efficiency of the MAC (%); m is the *p*-CP or *p*-NP mass (g), which is desorbed from the adsorbent and m_c is the remaining *p*-CP or *p*-NP mass on MAC before desorption (g). η is regeneration efficiency of the MAC (%), q_n and q_e are

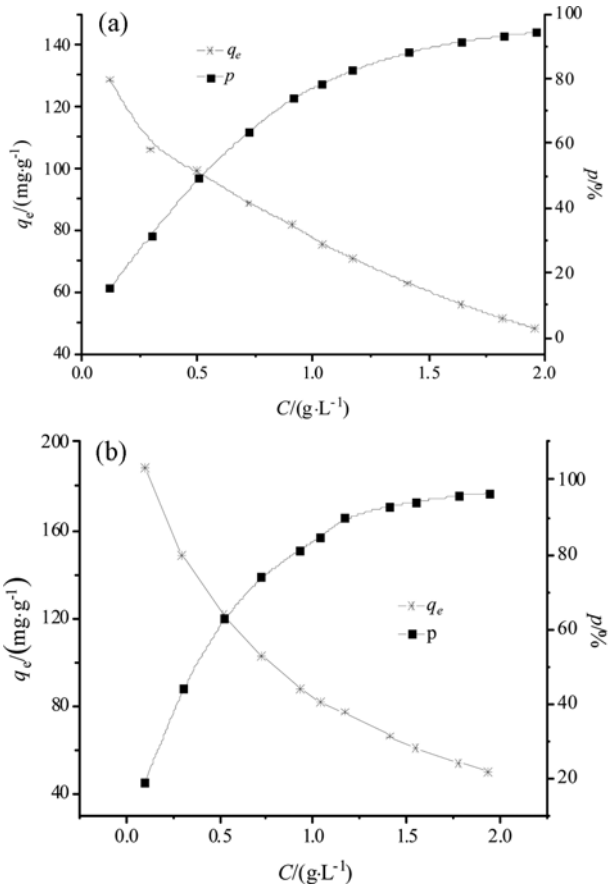

Fig. 1. Effect of adsorbent dose on adsorption quantity in single system (C_0=100 mg·L^{-1}, t=720 min): (a) *p*-CP on MAC; (b) *p*-NP on MAC.

the adsorption quantity of regenerative MAC for n (1, 2, 3) times and the fresh MAC in the same experimental conditions, respectively.

Desorption kinetic processes were conducted at different contact time.

RESULTS AND DISCUSSION

1. Adsorption Study

1-1. Effect of Adsorbent Dose on Adsorption Quantity

The effects of adsorbent dose on adsorption are illustrated in Fig. 1. It was seen that the adsorption amount of *p*-CP or *p*-NP decreased with the increase in adsorbent dose and the trends of *p*-CP and *p*-NP were same. The values of *p* increased with the increase in adsorbent dose and the trends were also same for *p*-CP and *p*-NP on MAC. The phenomenon was attributed to the number of adsorbate particles surrounding the per unit adsorbent. When the adsorbate concentration was constant, MAC particles with lower dose were surrounded by more adsorbate molecules, and the adsorbates were easier to act with the active sites on the adsorbent [26-28]. To achieve a relatively high removal efficiency with relatively few adsorbents, 1 g·L^{-1} was chosen in the following research.

1-2. Effect of Contact Time on Adsorption Quantity

Time is an important factor during the process. The effects of

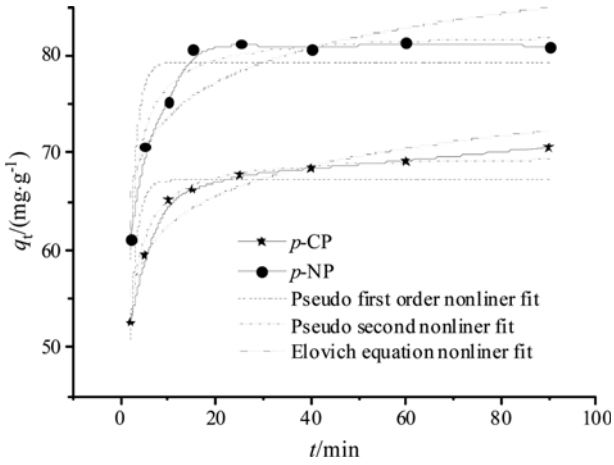

Fig. 2. Effect of contact time on adsorption quantity in single system and kinetic model fitted curves (C_0=100 mg·L^{-1}).

contact time on the adsorption process of single *p*-CP or *p*-NP system are shown in Fig. 2. It was observed that the adsorption process reached equilibrium quickly for both *p*-CP and *p*-NP onto MAC. Furthermore, the first 15 min exhibited rapid adsorption and then adsorbent gradually saturated. The reason was that large activated sites existed in the early stage and gradually decreased during the adsorption process [29-32]. The experimental data also showed that the equilibrium time for *p*-CP and *p*-NP in single system was 40 min and 25 min, respectively. The difference might be due to the electron withdrawing groups of *p*-CP and *p*-NP while the molecular sizes of *p*-CP and *p*-NP were close [30,33]. It was reported that the adsorption process of *p*-CP and *p*-NP followed the donor-acceptor mechanism. Electron density of the benzene ring was reduced by electron withdrawing group and the nitro group was reduced more than chloro group. Based on donor-acceptor mechanism, substituted phenols with lower electronic density were more easily combined with MAC, which could provide electrons [34]. Besides, 60 min was chosen as the equilibrium time.

To explore the adsorption process of *p*-CP and *p*-NP, various kinetic models are applied [35-37]. The formula expressions of kinetic models are listed in Table 1 and the fitting results by nonlinear regressive method are shown in Fig. 2 and Table 2. The determined coefficient (R^2) and the sum of the squared (SSE) are used to estimate the applicability of the used kinetic models. Elovich equation and pseudo-first-order kinetic model were not suitable to fit the kinetic process as there were lower values of R^2 and higher values of SSE. It was clear that the pseudo-second-order kinetic model was more suitable to describe the adsorption kinetic process. The fitting value of q_e from this model was close to the experimental value, further proving that pseudo-second-order kinetic model was more suitable to predict the equilibrium adsorption quantity. This suggested that chemisorption was predominant and the process involved valence forces through sharing or exchange of electrons [38].

1-3. Effect of Initial pH on Adsorption Quantity

The initial pH of the solution affects the existence of phenols, thereby affecting the adsorption efficiency. It is indispensable to study the effect of initial pH value on adsorption process, and the

Table 1. Adsorption isotherm models and dynamic models: description and nomenclature

Model	Nonlinear form	Nomenclature
Dynamic model		
Pseudo-first-order	$q_t = q_e(1-e^{-k_1 t})$	k_1 (min^{-1}) and k_2 ($g \cdot mg^{-1} \cdot min^{-1}$) were the rate constants of pseudo-first-order and pseudo-second-order, respectively; q_e ($mg \cdot g^{-1}$) and q_t ($mg \cdot g^{-1}$) were the adsorption capacity at equilibrium and at time t (min); $t_{1/2}$ is the time for the adsorption of half amount of adsorbate.
Pseudo-second-order	$q_t = \frac{k_2 q_e^2 t}{1+k_2 q_e t}$	
Elovich equation	$t_{1/2} = \frac{1}{k_2 q_e}$	A and B are constants.
Isotherm model	$q_t = A + B\ln t$	
Langmuir	$q_e = \frac{q_m K_L c_e}{1+K_L c_e}$	q_m ($mg \cdot g^{-1}$) is the monolayer maximum adsorption quantity; K_L ($L \cdot mg^{-1}$) is Langmuir constant related to binding energy.
Freundlich	$q_e = K_F c^{1/n}$	K_F ($L \cdot g^{-1}$) and n are Freundlich constant depending on temperature.
Koble-Corrigan	$q_e = \frac{AC_e^n}{1+BC_e^n}$	A, B and n are parameters.
Temkin	$q_e = A + B\ln C_e$	A and B are Temkin constant.

Table 2. Parameters of three kinetic models for *p*-CP and *p*-NP adsorption (303 K)

Pseudo-first-order kinetic model					
	$q_{e(exp)}$/($mg \cdot g^{-1}$)	$q_{e(theo)}$/($mg \cdot g^{-1}$)	k_1/(min^{-1})	R^2	SSE
p-CP	69.2	67.0±1.2	0.711±0.094	0.753	51.8
p-NP	81.4	79.3±1.4	0.681±0.087	0.781	70.4
Pseudo-second-order kinetic model					
	$q_{e(exp)}$/($mg \cdot g^{-1}$)	$q_{e(theo)}$/($mg \cdot g^{-1}$)	k_2/($g \cdot mg^{-1} \cdot min^{-1}$)	R^2	SSE
p-CP	69.2	69.2±0.4	0.00207±0.00014	0.981	3.90
p-NP	81.4	82.4±0.7	0.00167±0.00016	0.966	10.9
Elovich equation					
	A	B	R^2	SSE	
p-CP	52.5±2.0	4.30±0.65	0.861	29.2	
p-NP	61.9±3.2	5.10±1.02	0.774	72.7	

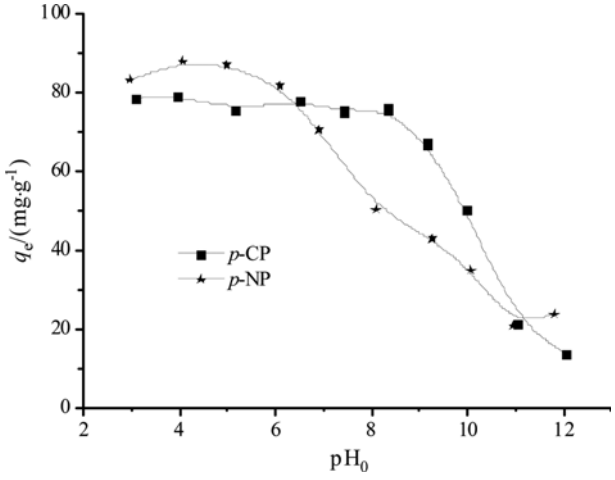

Fig. 3. Effect of pH on adsorption quantity in single system (C_0=100 mg·L^{-1}, adsorbent dose=1 g·L^{-1}, t=60 min).

results are shown in Fig. 3. With the increase in initial pH, the adsorption capacity of *p*-CP changed little at first but decreased sharply after pH 9.15. The initial pH had the same influence for *p*-NP on MAC, and the turning point was 6.09. The adsorption of *p*-CP and *p*-NP on MAC was strongly pH dependent; the pK_a values were 9.37 and 7.15, respectively. When the pH of solution is over the pK_a of phenols, phenols are mainly present in the negative phenolate ion. However, they are present in the neutral molecular form at solution pH below pK_a. Repulsion between phenols and MAC occurred when the solution pH was greater than both the pK_a of phenols and the pH_{zpc} of MAC [39]. Some substituted phenols exist in the form of negative ions when the solution pH is slightly below pK_a and the solubility of negative phenolate ions is greater than the molecule, but this is also a disadvantage of phenols adsorption [40,41]. The experimental facts also showed that molecule interaction was major between *p*-CP or *p*-NP and MAC. Thereby, the molecular interactions, such as hydrogen bonding,

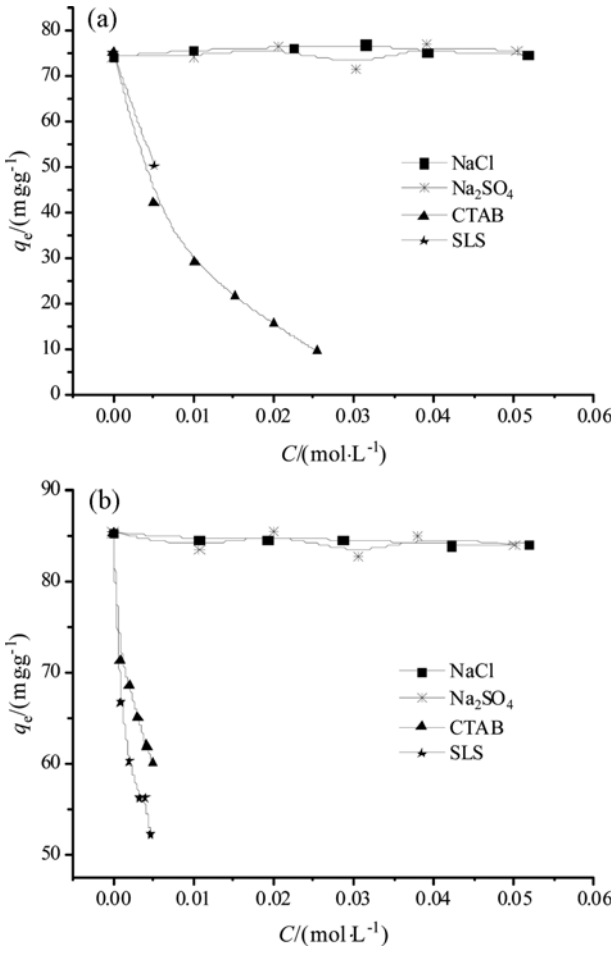

Fig. 4. Effect of coexisting ions on adsorption quantity in single system (C_0=100 mg·L^{-1}, t=60 min): (a) *p*-CP on MAC; (b) *p*-NP on MAC.

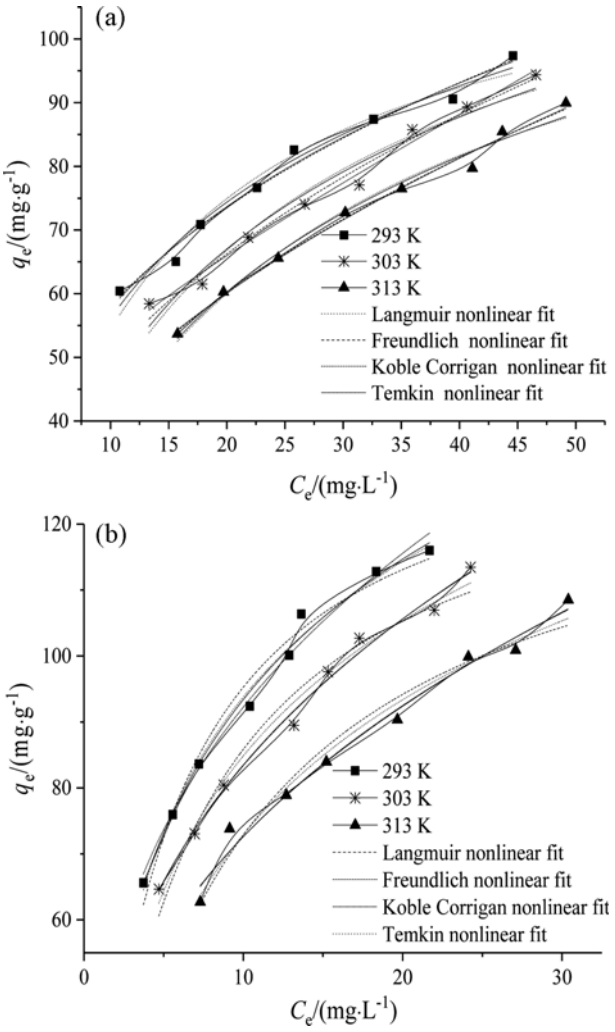

Fig. 5. Effect of adsorption temperature and adsorbate concentration on adsorption quantity in single system and adsorption isotherms nonlinear fitted curves (C_0=70-140 mg·L^{-1}, t=60 min): (a) *p*-CP on MAC; (b) *p*-NP on MAC.

hydrophobic interaction and van der Waals force were the possible factors to affect the adsorption process [42]. The solution initial pH of *p*-CP and *p*-NP were 6.49 and 6.09, and the solution pH was not adjusted for the following experiments.

1-4. Effect of Coexistence on Adsorption Quantity

To explore the effect of coexistence in actual water and further investigate the adsorption mechanism, various concentrations of coexistence (NaCl, Na_2SO_4, CTAB and SLS) were added into the suspension; the results of single system are exhibited in Fig. 4. It is reported that the adsorption quantity becomes lower at higher salt concentration if electrostatic interactions or ion exchange exists between adsorbents and adsorbates [43]. In Fig. 4, neither NaCl nor Na_2SO_4 had any apparent effect on the adsorption quantity, which further confirmed that the binding of *p*-CP and *p*-NP onto MAC was in the form of molecules. Moreover, the presence of CTAB and SLS greatly influenced the adsorption quantity, indicating the existence of hydrogen bonding force during the adsorption process [44,45].

1-5. Effect of *p*-CP or *p*-NP Concentration and Temperature on Adsorption Quantity

The effects of adsorbate concentration and temperature on the equilibrium adsorption were studied, with experimental results illustrated in Fig. 5. The q_e values of *p*-CP and *p*-NP increased with the increase in adsorbate concentration and presented a similar trend. There was higher adsorption capacity for *p*-CP onto surface of MAC. Values of q_e were up to 97.3, 94.4, 90.0 mg·g^{-1} for *p*-CP and 116, 113, 108 mg·g^{-1} for *p*-NP at 293, 303, and 313 K, respectively. It was due to the higher number of adsorbate surrounding the active sites of MAC with the increase in *p*-CP or *p*-NP concentration. Hence, the adsorption reaction was more sufficient [29]. The figures also demonstrated that the adsorption capacity decreased with the increase in temperature. This phenomenon suggested that the adsorption process was exothermic and was more inclined to physical adsorption [46].

To explain the adsorption mechanism, Langmuir, Freundlich, Temkin, and Koble-Corrigan models were used to fit the adsorption isotherm curves using nonlinear regressive method. The models used are also listed in Table 1. The fitting parameters, the determined coefficients (R^2) and the sum of squares of errors (SSE) are in Table 3

Table 3. The parameters of isotherms at different temperatures for *p*-CP and *p*-NP

***p*-CP**					
Langmuir					
T/K	K_L/(L·mg^{-1})	$q_{e(exp)}$/(mg·g^{-1})	$q_{m(theo)}$/(mg·g^{-1})	R^2	SSE
293	0.0825±9.6×10^{-3}	97.3	120±5	0.965	34.5
303	0.0542±8.5×10^{-3}	94.4	128±8	0.951	50.3
313	0.0442±5.5×10^{-3}	90.0	128±5	0.980	19.1
Freundlich					
T/K	K_F	1/n	R^2	SSE	
293	26.5±1.6	0.341±0.018	0.982	18.1	
303	19.3±1.5	0.412±0.022	0.981	19.3	
313	16.2±1.0	0.437±0.018	0.989	9.93	
Koble-Corrigan					
T/K	A/(L·mg^{-1})	B/(L·mg^{-1})	n	R^2	SSE
293	25.6±5.5	0.0551±0.1728	0.411±0.280	0.978	17.9
303	2.58±3.80	−0.971±0.119	0.0149±0.0169	0.984	13.2
313	17.3±3.1	−0.0513±0.2426	0.361±0.285	0.987	9.79
Temkin					
T/K	A	B	R^2	SSE	
293	−4.61±4.85	26.4±1.5	0.977	22.7	
303	−22.5±7.5	29.9±2.3	0.961	39.6	
313	−31.7±5.2	30.7±1.5	0.983	15.5	
***p*-NP**					
Langmuir					
T/K	K_L/(L·mg^{-1})	$q_{e(exp)}$/(mg·g^{-1})	$q_{m(theo)}$/(mg·g^{-1})	R^2	SSE
293	0.0217±0.0211	116	139±4	0.977	44.6
303	0.0170±0.0201	113	136±5	0.968	57.6
313	0.0121±0.0148	108	133±5	0.964	51.8
Freundlich					
T/K	K_F	1/n	R^2	SSE	
293	43.7±1.8	0.325±0.016	0.985	29.3	
303	38.1±1.4	0.341±0.013	0.991	16.8	
313	32.5±1.9	0.349±0.019	0.981	27.1	
Koble-Corrigan					
T/K	A	B	n	R^2	SSE
293	43.8±4.4	0.205±0.063	0.578±0.172	0.988	20.1
303	38.4±2.6	0.030±0.201	0.366±0.181	0.988	16.8
313	32.2±4.5	−0.038±0.399	0.316±0.308	0.977	27.1
Temkin					
T/K	A	B	R^2	SSE	
293	25.5±2.9	29.7±1.2	0.988	22.6	
303	16.7±3.7	29.6±1.4	0.984	28.4	
313	5.02±4.89	39.5±1.7	0.977	33.6	

for *p*-CP and for *p*-NP, respectively. The fitted curves are also shown in Fig. 5.

It was observed from Table 3 that there were higher values of R^2 and lower values of SSE from Freundlich model fitted results for both *p*-CP and *p*-NP. These showed that the Freundlich model was most suitable for describing the adsorption process. The adsorption coefficient K_F decreased with the increase in temperature, which indicated that the decrease in temperature was beneficial to the adsorption process. But the trend of 1/n was in contrast. The fitting parameters 1/n were between 0.3 and 0.5, illustrating easy adsorption. The Freundlich model is an empirical formula used to describe the adsorption process of high concentration adsorbates on heterogeneous surfaces [47].

For Langmuir model, values of K_L decreased with the increase in temperature for both *p*-CP and *p*-NP adsorption. There were lower values of R^2 and higher values of SSE. Furthermore, the val-

ues of q_m from Langmuir model were not closer to values of q_e from experiments at all conditions. So this model was not suitable to fit the equilibrium process.

Based on similar analysis, the Koble-Corrigan model was also available to fit the equilibrium process, but the Temkin model was not suitable to predict the process.

Linear fitting method is also done for relation of q_e and C_e to explore the adsorption mechanism. The results are shown in Table 4 and Fig. 6, respectively. From Table 4, the values of R^2 were all above 0.929 at experimental conditions. The fitting results indicated that the distribution effect existed in the adsorption process as there was better linear relation between q_e and C_e (similar to Henry's Law). Another study showed that there was better linear relation between q_e and C_0 about methylene blue adsorption onto surface of chaff [48].

Table 4. The relation between the amount of *p*-CP and *p*-NP adsorbed onto per unit mass of MAC (q_e) and *p*-CP or *p*-NP equilibrium concentration (C_e)

Adsorbate	T/K	Adsorption equation	R^2
p-CP	293	q_e=1.07 C_e+51.0	0.959
	303	q_e=1.13 C_e+43.2	0.987
	313	q_e=1.04 C_e+39.4	0.983
p-NP	293	q_e=2.80 C_e+61.4	0.929
	303	q_e=2.41 C_e+57.2	0.964
	313	q_e=1.04 C_e+39.4	0.966

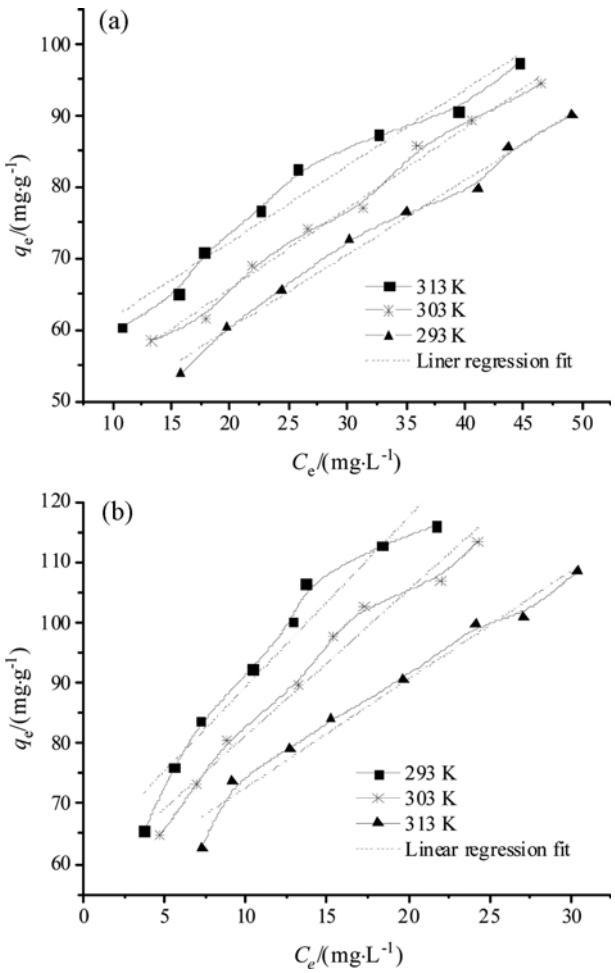

Fig. 6. Linear fitted curves of *p*-CP (a) and *p*-NP (b) on MAC at various temperatures (C_0=70-140 mg·L^{-1}, t=60 min).

2. Diffusion Processes

To assess the diffusion process responsible for the adsorption of *p*-CP and *p*-NP on MAC, attempts were made to calculate the coefficients of the process. Assuming spherical geometry, the rate constants of the adsorption process can be related with the pore diffusion coefficient (D_p) and the film diffusion coefficient (D_f) independently [49]. It is vital to calculate the pore diffusion coefficients (D_p) and the film diffusion coefficient (D_f) for the adsorption process of *p*-CP and *p*-NP on MAC [50,51].

$$t_{1/2}=\frac{1}{k_2 q_e} \tag{7}$$

$$D_p=\frac{0.03 r_0^2}{t_{1/2}} \tag{8}$$

$$D_f=\frac{0.23 r \varepsilon}{t_{1/2}}\times\frac{q_e}{C_0} \tag{9}$$

where C_0 is the initial concentration and $t_{1/2}$ is the time for the adsorption of half amount of adsorbate at equilibrium (values of k_2 and q_e obtained from Table 2), r_0 (cm) is the radius of adsorbent and ε the film thickness (10^{-3} cm) [49,50]. The adsorbent was assumed to be in spherical form and the radius of the adsorbent was considered as 1 μm, which was based on the SEM analysis [19]. If pore diffusion is rate limiting, values of D_p may be in the range 10^{-11} to 10^{-13} cm^2·s^{-1}. If film diffusion is the rate-determining step, the value of D_f should be in the range 10^{-6} to 10^{-8} cm^2/s.

By considering the relative data and the respective rate constants, pore and film diffusion coefficients were obtained. The values of D_p was found to be 7.02×10^{-8} cm^2·s^{-1} and 6.88×10^{-8} cm^2·s^{-1} for *p*-CP and *p*-NP on MAC, respectively. The values of D_p were both on the order of 10^{-8}, which indicated that the pore diffusion was not significant [45]. The values of D_f were 1.37×10^{-6} cm^2·s^{-1} and 1.56×10^{-6} cm^2·s^{-1} for *p*-CP and *p*-NP on MAC, respectively. It clearly showed that removal of *p*-CP and *p*-NP on MAC was controlled by film diffusion process since coefficient values were around 10^{-6} cm^2·s^{-1}. Compared to values of D_p and D_f, film diffusion was faster than pore diffusion.

3. Thermodynamic Studies

The thermodynamics parameters such as Gibbs free energy (ΔG^0), enthalpy (ΔH^0) and entropy (ΔS^0) could be calculated by the following formula [52].

$$K_c'=\frac{C_{ad,e}}{C_e} \tag{10}$$

$$\Delta G^0=-RT\ln K_c' \tag{11}$$

$$\Delta G^0=\Delta H^0-T\Delta S^0 \tag{12}$$

where K_c' is apparent adsorption equilibrium constant. $C_{ad,e}$ represents the equilibrium concentration of adsorbate on the adsorbent. T is the experimental temperature (K) and R is universal gas

Table 5. Thermodynamic parameters of *p*-CP and *p*-NP adsorption on MAC

	ΔH/ (kJ·mol^{-1})	ΔS/ (J·mol^{-1}·K^{-1})	ΔG/(kJ·mol^{-1})		
			293 K	303 K	313 K
p-CP	−12.2	17.8	−7.03	−6.81	−6.67
p-NP	−17.6	28.9	−9.08	−8.95	−8.51

constant (8.314 J·mol^{-1}·K^{-1}). Values of ΔH^0 (kJ·mol^{-1}) and ΔS^0 (J·mol^{-1}·K^{-1}) are obtained by van't Hoff equation.

Thermodynamics parameters were calculated and listed in Table 5. The values of ΔG^0 for *p*-CP and *p*-NP on MAC at 293 K, 303 K and 313 K were all negative, and the absolute values of ΔG^0 decreased with the increase in temperature. It suggested spontaneity of reaction and unfavorable at higher temperature. All ΔG^0 values were between 0~−20 kJ·mol^{-1}, indicating a physical adsorption. The negative values of ΔH^0 implied the exothermic nature of reaction. The positive ΔS^0 values indicated an increased randomness at the solid-solution interface during the adsorption process [11].

4. Desorption and Regeneration Study

Good regenerative capacity is vital to an ideal adsorbent [53]. Desorption and regeneration experiments are performed, and the results are shown in Fig. 7. Among the methods of desorption, it was clearly seen that there was higher desorption and regeneration ability when 0.1 mol·L^{-1} and 0.01 mol·L^{-1} NaOH were used as desorption agents and the regeneration efficiency was above 91.2%. Under alkaline conditions, the surface of MAC and substituted phenols were negatively charged, which resulted in repulsion and facilitated the desorption process. This phenomenon was consistent with the effect of initial pH on the adsorption process. Considering environmental friendliness and regeneration capacity of adsorbent, 0.01 mol·L^{-1} NaOH was chosen as the desorbing solution for continuous desorption-adsorption studies; the results are shown in Fig. 8. It was clearly found that values of the regeneration efficiency of MAC (desorbed *p*-CP-MAC and *p*-NP-MAC) were all above 95.0% and 93.2% after three cycles, respectively. This phenomenon might be attributed to adsorption unsaturation and suggested that MAC had good reusability [20].

Kinetic desorption of *p*-CP-MAC and *p*-NP-MAC is studied, and the results are shown in Fig. 9. It was seen that the whole desorption process was very fast. The desorption efficiency reached 63.7% and 59.0% when the contact time was just 5 min. The desorption process reached equilibrium at 40 min and 60 min, and desorption efficiency was 71.4% and 68.3%, respectively. The higher

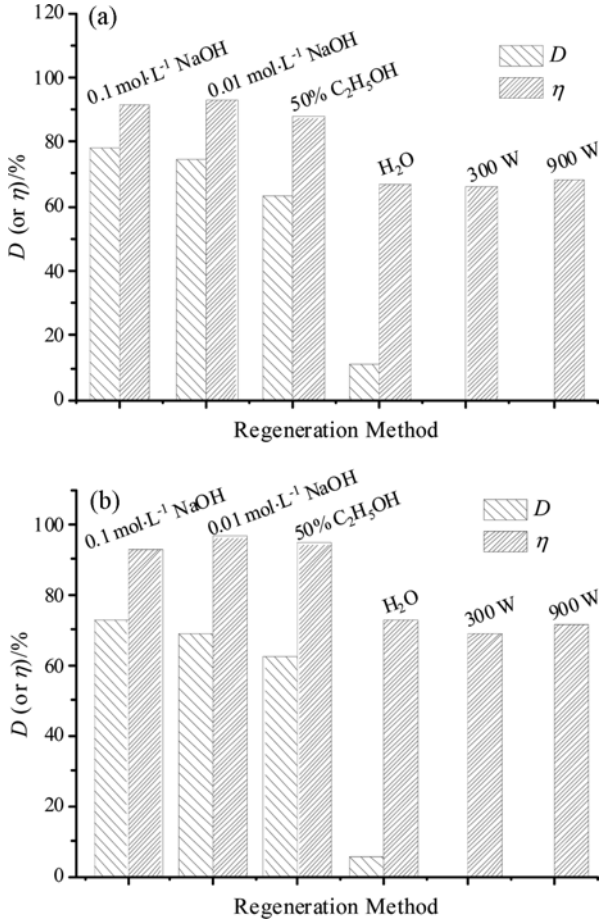

Fig. 7. Desorption efficiency and regeneration efficiency of various methods (C_0=100 mg·L^{-1}, t=60 min): (a) *p*-CP; (b) *p*-NP.

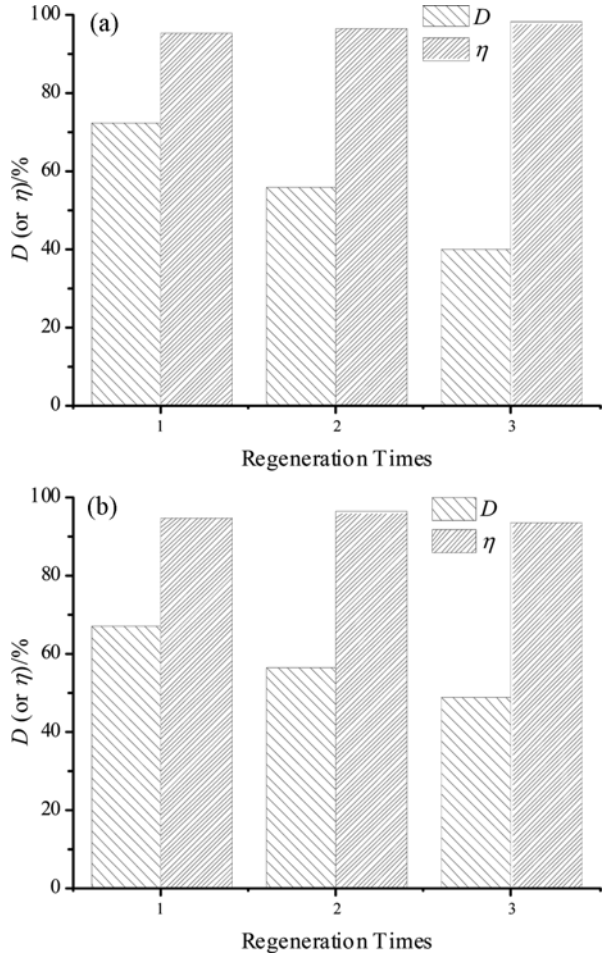

Fig. 8. Desorption efficiency and regeneration efficiency of three cycles (C_0=100 mg·L^{-1}, t=90 min): (a) *p*-CP; (b) *p*-NP.

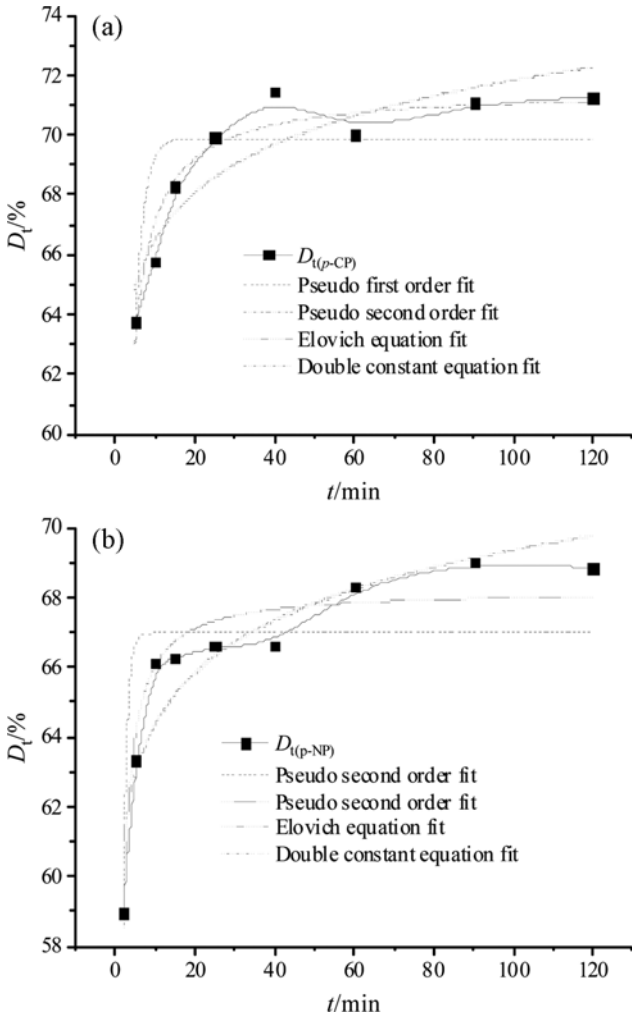

Fig. 9. Desorption of adsorbate from spent MAC and kinetic model fitted curves (desorbing solution: 0.01 mol·L^{-1} NaOH): (a) *p*-CP; (b) *p*-NP.

desorption efficiency indicated that binding force of *p*-CP and *p*-NP on MAC was relatively weak [54].

Different kinetic models were applied on desorption kinetic process to clarify the desorption mechanism (see Fig. 9 and Table 6). Values of R^2 were in the order of pseudo-second-order kinetic model>Elovich equation>double constant equation>pseudo-first-order kinetic model, while values of SSE were in the order of pseudo-second-order kinetic model<Elovich equation<double constant equation<pseudo-first-order kinetic model for *p*-CP and *p*-NP, respectively. Furthermore, values of D_t from the pseudo-second-order kinetic model were closer to values of D_t from pseudo-first-order kinetic model for *p*-CP and *p*-NP, respectively. However, the fitted curves from pseudo-first-order kinetic model were closer to experimental curves. So it was concluded that pseudo-second-order kinetic model had the best evaluation results.

5. Competitive Adsorption of *p*-CP and *p*-NP on MAC in Binary System

5-1. Effect of *p*-CP or *p*-NP Adsorption on MAC with the Presence of *p*-NP or *p*-CP

In the competition system, the concentration of *p*-CP or *p*-NP was fixed to 100 mg·L^{-1} while the concentration of *p*-NP or *p*-CP was changed from 70 mg·L^{-1} to 140 mg·L^{-1}. The results are illustrated in Fig. 10. Note that the presence of *p*-NP or *p*-CP affected the adsorption quantity of *p*-CP or *p*-NP. Furthermore, the influence was more significant with the increased concentration in co-solute [23]. In addition, the q_e values of *p*-CP decreased from 0.447 mmol·g^{-1} to 0.367 mmol·g^{-1} (decreased 17.9%) at the presence of *p*-NP, while the q_e values of *p*-NP decreased from 0.463 mmol·g^{-1} to 0.423 mmol·g^{-1} (decreased 8.80%) at the presence of *p*-CP. This results demonstrated that the presence of *p*-NP had a greater influence on the adsorption quantity of *p*-CP and *p*-NP had a strong affinity with MAC than *p*-CP. It was inferred that stronger withdrawing group and lower water solubility of *p*-NP contributed to the results (solubility at 298 K, *p*-CP 27 g·L^{-1} and *p*-NP 17 g·L^{-1}) [25,34,55].

Table 6. Desorption kinetics for *p*-CP-MAC and *p*-NP-MAC (303 K)

Pseudo-first-order kinetic model					
Adsorbate	$D_{t(theo)}$/(%)	$D_{t(exp)}$/(%)	k_1/(min^{-1})	R^2	SSE
p-CP	69.9±0.7	71.0	0.464±0.057	0.574	20.3
p-NP	67.0±0.6	69.0	1.04±0.11	0.686	22.0
Pseudo-second-order kinetic model					
Adsorbate	$D_{t(theo)}$/(%)	$D_{t(exp)}$/(%)	k_2/(g·mg^{-1}·min^{-1})	R^2	SSE
p-CP	71.5±0.4	71.0	0.0210±0.0058	0.919	3.86
p-NP	68.2±0.3	69.0	0.0443±0.0048	0.935	4.55
Elovich equation					
Adsorbate	A	B	R^2	SSE	
p-CP	61.1±1.5	2.33±0.42	0.813	8.90	
p-NP	59.3±1.0	0.460±0.300	0.865	9.43	
Double constant equation					
Adsorbate	A	K_s	R^2	SSE	
p-CP	61.5±1.4	0.0335±0.0063	0.802	9.43	
p-NP	59.6±1.0	0.0328±0.0048	0.853	10.3	

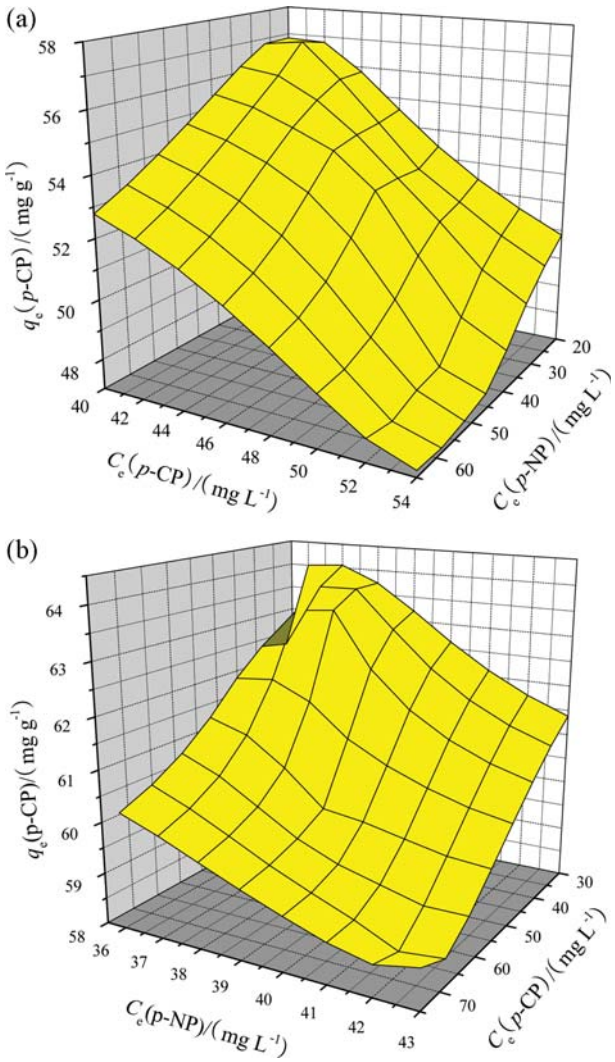

Fig. 10. The adsorption quantity for *p*-CP and *p*-NP at different equilibrium concentration in binary system ($C_{0,p\text{-CP or }p\text{-NP}}$=100 mg·L^{-1}, $C_{0,p\text{-NP or }p\text{-CP}}$=70-140 mg·L^{-1}, t=90 min).

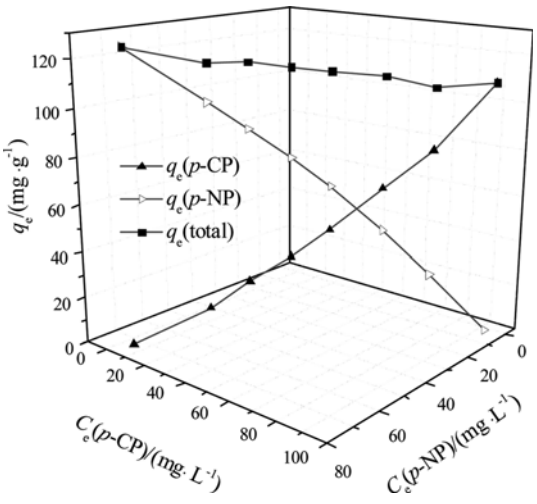

Fig. 11. The effect of both *p*-CP and *p*-NP in existence on the adsorptive capacity of MAC ($C_{0,total}$=200 mg·L^{-1}, t=60 min).

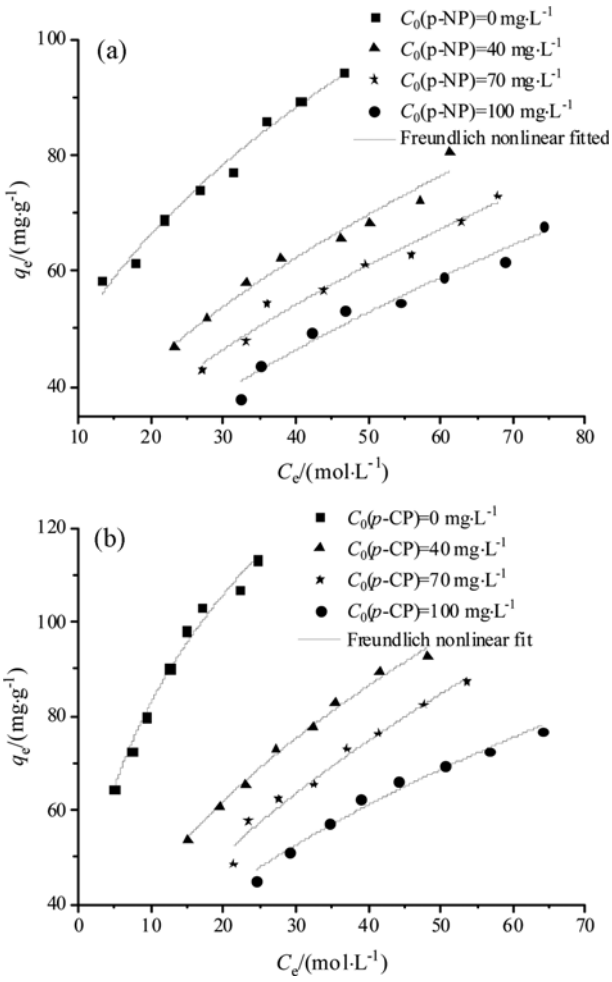

Fig. 12. Freundlich model fitted curves for single and binary systems (a) $C_{0,p\text{-CP}}$=70-140 mg·L^{-1}, $C_{0,p\text{-NP}}$=0, 40, 70, 100 mg·L^{-1}, t=60 min); (b) $C_{0,p\text{-NP}}$=70-140 mg·L^{-1}, $C_{0,p\text{-CP}}$=0, 40, 70, 100 mg·L^{-1}, t=60 min).

5-2. Competitive Adsorption of *p*-CP and *p*-NP at a Fixed Total Concentration

To study the effect of *p*-CP and *p*-NP coexistence on the total adsorptive capacity of MAC, the total concentration was fixed (200 mg·L^{-1}) and each constituent was changed. The results (see Fig. 11) results that the total adsorption capacity slightly decreased with the decrease of *p*-NP concentration in binary system. It suggested that MAC prefers to adsorb *p*-NP. Furthermore, the q_e values of *p*-CP and *p*-NP in binary system were lower than those in single system. The results further proved that competitive adsorption existed in bi-component system.

5-3. Freundlich Model Fitting for Single and Binary Systems

To figure out the adsorption behavior of *p*-CP and *p*-NP, the Freundlich model was selected to fit the experimental data. The fitting results for single and binary systems are shown in Fig. 12 and Table 7, respectively. Values of R^2 and SSE from the fitting results showed that the Freundlich model was suitable for describing the adsorption process and indicated that the process was multi-layer adsorption on an uneven surface [56]. In the single system, it was obvious that the adsorption capacity of *p*-NP was higher

Table 7. Parameters for *p*-CP and *p*-NP adsorption using Freundlich model

Adsorbate	C_0 (*p*-NP)	K_F	1/n	R^2	SSE
p-CP	0	19.3±1.5	0.412±0.022	0.981	19.3
	40	9.64±1.35	0.505±0.037	0.966	24.2
	70	7.53±1.07	0.535±0.036	0.970	17.9
	100	5.26±0.99	0.590±0.047	0.959	23.1
p-NP	0	36.6±1.8	0.354±0.018	0.983	29.9
	40	14.6±0.8	0.482±0.016	0.993	8.28
	70	9.34±1.23	0.564±0.036	0.973	27.0
	100	8.93±1.08	0.521±0.032	0.976	16.8

than *p*-CP as the K_F values of *p*-NP and *p*-CP were 36.6 and 19.3, respectively. Furthermore, values of K_F in single system were still larger than values of K_F in binary system with the same coexisting solute concentration [50]. For one solute (in binary system), values of K_F became lower, while values of 1/n became larger with the increase in *p*-NP or *p*-CP concentration (except for *p*-NP at 70 mg/L *p*-CP). All the results showed that *p*-NP was in dominant position during adsorption process.

CONCLUSION

MAC was used to remove *p*-CP and *p*-NP and the adsorption process in single and binary systems was presented. The initial solution pH and the existing surfactant strongly affected the adsorption capacity in the single system. Furthermore, there was competitive adsorption in the binary system, and *p*-NP adsorbed on MAC more easily than *p*-CP. Freundlich model better fit the equilibrium results, and the process was spontaneous and exothermic. The spent MAC can be effectively regenerated using NaOH solution. In addition, the adsorption mechanism of *p*-CP and *p*-NP on MAC was presumed to be hydrogen-bonding, electron donor-acceptor and π-π interactions. MAC is effective for adsorbing *p*-CP and *p*-NP from solution.

REFERENCES

1. M. Anbia and S. Khoshbooei, *J. Nanostruct. Chem.*, **5**, 139 (2015).
2. B. Koubaissy, J. Toufaily, M. El-murr, T. Hamieh, P. Magnoux and G. Joly, *Phys. Procedia*, **21**, 220 (2011).
3. L. R. Rad, I. Haririan and F. Divsar, *Spectrochim. Acta A*, **136**, 423 (2015).
4. C. A. Acosta, C. Pasquali, G. Paniagua, R. M. Garcinuño and P. F. Hernando, *Environ. Pollut.*, **236**, 265 (2018).
5. C. Borras, T. Laredo and B. R. Scharifker, *Electrochim. Acta*, **48**, 2775 (2003).
6. H. Ozaki and H. Li, *Water Res.*, **36**, 123 (2002).
7. Y. Li and K. C. Loh, *J. Appl. Polym. Sci.*, **105**, 1732 (2010).
8. S. H. Lin and C. S. Wang, *J. Hazard. Mater.*, **90**, 205 (2002).
9. C. Sheng, X. M. Zheng, K. Fei, G. H. Wu, L. L. Luo, G. Yong, H. L. Liu, W. Ying, H. X. Yu and Z. G. Zou, *Mater. Chem. Phys.*, **129**, 1184 (2011).
10. J. Wu and H. Q. Yu, *J. Hazard. Mater.*, **137**, 498 (2006).
11. J. Su, H. F. Lin, Q. P. Wang, Z. M. Xie and Z. L. Chen, *Desalination*, **269**, 163 (2011).
12. M. Salman, M. Athar and U. Farooq, *Rev. Environ. Sci. Bio.*, **14**, 211 (2015).
13. J. L. Wang and C. Chen, *Biotechnol. Adv.*, **17**, 195 (2009).
14. A. Bhatnagar, W. Hogland, M. Marques and M. Sillanpää, *Chem. Eng. J.*, **219**, 499 (2013).
15. P. Cañizares, M. Carmona, O. Baraza, A. Delgado and M. A. Rodrigo, *J. Hazard. Mater.*, **131**, 243 (2006).
16. N. Yang, S. M. Zhu, D. Zhang and S. Xu, *Mater. Lett.*, **62**, 645 (2008).
17. S. Singh, *Res. J. Chem. Sci.*, **6**, 361 (2015).
18. S. Han, F. Zhao, J. Sun, B. Wang, R. Y. Wei and S. Q. Yan, *J. Magn. Magn. Mater.*, **341**, 133 (2013).
19. Y. C. Rong, H. Li, L. H. Xiao, Q. Wang, Y. Y. Hu, S. S. Zhang and R. P. Han, *Desalin. Water. Treat.*, **106**, 273 (2018).
20. B. Kakavandi, M. Jahangiri-rad, M. Rafiee, A. R. Esfahani and A. A. Babaei, *Micropor. Mesopor. Mater.*, **231**, 192 (2016).
21. V. L. Lassalle, R. D. Zysler and M. L. Ferreira, *Mater. Chem. Phys.*, **130**, 624 (2011).
22. L. C. A. Oliveira, R. Rios, J. D. Fabris, V. Garg, K. Sapag and R. M. Lago, *Carbon*, **40**, 2177 (2002).
23. A. Tóth, A. Törőcsik, E. Tombácz and K. László, *J. Colloid Interface Sci.*, **387**, 244 (2012).
24. Q. M. Wei and T. Nakato, *Micropor. Mesopor. Mater.*, **96**, 84 (2006).
25. E. F. Mohamed, C. Andriantsiferana, A. M. Wilhelm and H. Delmas, *Environ. Technol.*, **32**, 1325 (2011).
26. Y. B. Jiao, D. L. Han, Y. Z. Lu, Y. C. Rong, L. Y. Fang, Y. L. Liu and R. P. Han, *Desalin. Water. Treat.*, **77**, 247 (2017).
27. T. Zhou, L. Y. Fang, X. W. Wang, M. Y. Han, S. S. Zhang and R. P. Han, *Desalin. Water Treat.*, **70**, 294 (2017).
28. I. K. Battisha, H. H. Afify and M. Ibrahim, *J. Magn. Magn. Mater.*, **306**, 211 (2006).
29. J. Y. Song, W. H. Zou, Y. Y. Bian, F. Y. Su and R. P. Han, *Desalination*, **265**, 119 (2011).
30. R. D. Zhang, J. H. Zhang, X. N. Zhang, C. C. Dou and R. P. Han, *J. Taiwan Inst. Chem. E.*, **45**, 2578 (2014).
31. N. Li, J. Chen and Y. P. Shi, *Anal. Chim. Acta*, **949**, 23 (2017).
32. G. Mihoc, R. Ianoş and C. Păcurariu, *Water Sci. Technol.*, **69**, 385 (2014).
33. B. Zhang, F. Li, T. Wu, D. J. Sun and Y. J. Li, *Colloids Surf., A.*, **464**, 78 (2015).
34. S. K. Srivastava and R. Tyagi, *Water Res.*, **29**, 483 (1995).
35. F. Zhang, Z. Wei, W. N. Zhang and H. Y. Cui, *Spectrochim. Acta A*, **182**, 116 (2017).
36. Y. S. Ho and G. Mckay, *Process Biochem.*, **34**, 451 (1999).
37. C. W. Cheung, J. F. Porter and G. Mckay, *Sep. Purif. Technol.*, **19**, 55 (2000).
38. B. H. Hameed and A. A. Rahman, *J. Hazard. Mater.*, **160**, 576 (2008).
39. A. E. Ofomaja and E. I. Unuabonah, *Carbohydr. Polym.*, **83**, 1192 (2011).
40. A. E. Vasu, *E-J. Chem.*, **5**, 224 (2012).
41. I. A. Bello, M. A. Oladipo, A. A. Giwa and D. O. Adeoye, *Int. J. Basic Appl. Sci.*, **2**, 79 (2013).
42. J. M. Li, X. G. Meng, C. W. Hu and J. Du, *Bioresour. Technol.*, **100**, 1168 (2009).

43. H. A. Arafat, M. Franz and N. G. Pinto, *Langmuir*, **15**, 5997 (1999).
44. K. Yang, Q. Jing, W. Wu, L. Zhu and B. Xing, *Environ. Sci. Technol.*, **44**, 681 (2010).
45. M. Ahmaruzzaman and D. K. Sharma, *J. Colloid Interface Sci.*, **287**, 14 (2005).
46. K. A. Halhouli, N. A. Darwish and Y. R. Y. Al-Jahmany, *Sep. Sci. Technol.*, **32**, 3027 (1997).
47. G. Crini, *Dyes Pigm.*, **77**, 415 (2008).
48. R. P. Han, Y. F. Wang, P. Han, J. Shi, J. Yang and Y. S. Lu, *J. Hazard. Mater.*, **137**, 550 (2006).
49. M. Chabani, A. Amraneb and A. Bensmaili, *Chem. Eng. J.*, **125**, 111 (2006).
50. T. S. Anirudhan and M. Ramachandran, *J. Water Process Eng.*, **1**, 46 (2014).
51. C. Y. Chang, W. T. T. Sai, C. H. Ing and C. H. Chang, *J. Colloid Interface Sci.*, **260**, 273 (2003).
52. Y. Fan, R. F. Yang, Z. M. Lei, N. Liu, J. L. Lv, S. R. Zhai, B. Zhai and L. Wang, *Korean J. Chem. Eng.*, **33**, 1416 (2016).
53. T. Zhou, W. Z. Lu, L. F. Liu, H. M. Zhu, Y. B. Jiao, S. S. Zhang and R. P. Han, *J. Mol. Liq.*, **211**, 909 (2015).
54. M. L. Nguyen and R. S. Juang, *Biotechnol. Bioproc. E.*, **20**, 614 (2015).
55. J. M. Chern and Y. W. Chien, *Water Res.*, **37**, 2347 (2003).
56. S. R. Ha and S. Vinitnantharat, *Environ. Technol.*, **21**, 387 (2000).